IT ALL COMES TOGETHER: EXAMINING STRUCTURAL ELEMENTS OF THE GLMS RIBOZYME IN *T. thermophilus*

by
James Cameron

A thesis submitted to Johns Hopkins University in conformity with the requirements for the degree of Master of Science

Baltimore, Maryland
April, 2017

Abstract

The discovery of catalytic RNA shifted the traditional view of RNA as a passive messenger to one in which RNA occupied a regulatory role in cellular processes. Self-cleaving ribozymes and metabolite sensing riboswitches emerged as widespread and evolutionarily conserved mechanisms of controlling gene expression. One of these metabolite binding ribozymes resides in the 5' UTR of an essential gene, glmS which encodes an enzyme involved in cell biosynthesis. A downstream metabolic product of glmS synthase, glucosamine-N-6- phosphate (GlcN6P), binds the *glmS* ribozyme resulting in self-cleavage of the 5' leader sequence and degradation of the mRNA transcript. Thus, the *glmS* ribozyme acts as the key component in a negative feedback loop, tightly regulating expression of GlmS synthase. Here I investigated the significance of an additional module within the *glmS* ribozyme in a Gram-negative thermophilic bacterium, *Thermus. thermophilus.* This additional module contains a series of structures with RNA tertiary interaction motifs, which increase the stability of the RNA. Given the high temperature environment in which *T. thermophilus* resides, the presence of additional RNA tertiary motifs in a highly-conserved ribozyme like *glmS* suggests that the additional module is necessary for function. My data indicate that mutations to tertiary interactions within the additional module disrupt proper folding, leading to a loss of stability and a decrease in function. Rather than stabilize the core of the ribozyme at high temperature, I found that the additional module assists in folding the ribozyme into a functional state. A deeper understanding of the *glmS* ribozymes folded structure enhances our understanding of the active site of the ribozyme and the mechanism of ligand

binding. A GlcN6P analog that could trigger self-cleavage would result in inhibition of the essential gene GlmS synthase. Such an analog would therefore have potential as a broad-spectrum antibiotic. Development of such a drug requires detailed knowledge of the ribozymes folded structure, and this work contributes toward that task.

Reader: Sarah Woodson

Preface

This work represents the natural evolution of a long-term interest in regulatory mechanisms. I was always intrigued by the complexities of the regulation, particularly at the molecular level. Working in Sarah Woodson's laboratory provided me with an opportunity to apply that interest to an independent research project on ribozymes. Like riboswitches, ribozymes function as key elements in regulatory networks, moderating cellular response to internal or external stimulus. I decided to study the *glmS* ribozyme, which regulates cellular division, an essential process. In the presence small metabolite, *glmS* undergoes self-cleavage, preventing it's own translation. The mechanism of reaction is inherent in the shape, and therefore nucleic acid sequence, of the ribozyme. It is the best example of form meeting function that nature can devise, and encapsulates the elegance that first drew me to molecular biology.

Acknowledgements

I owe a debt of gratitude to Sarah Woodson not only for helping me in preparing this Thesis, but in preparing me to be in the position to even think about conducting an independent project. I came to you an untutored undergraduate who barely knew my left from my right scientifically. Over the last few years the time and effort you have put into my education has allowed me to embark upon this research project, and I am thankful for your continuous support. I would also like to thank the members of the Woodson lab for putting up with my incessant questions. Darrin Zhornacky and Andrew Santiago-Frangos have both been immeasurably patient and a great deal of fun to work with. Thank you.

Table of Contents

Tables

Table 1: Summary of MT and WT activity. Half maximal magnesium concentrations and maximum cleavage attained for each mutant.

Genotype	$[\mathbf{Mg}]_{1/2}$ mM (65 °C)	Maximum Cleavage (65°C)	$[\mathbf{Mg}]_{1/2}$ mM (42 °C)	Maximum Cleavage (42°C)
WT	6.4 ± 0.4	37%	4.4 ± 0.3	5%
ΔA72-A109	N/A	0%	N/A	0%
U95G	5.7 ± 0.3	33%	3.6 ± 1.1	11%
ΔA86-A87	12.9 ± 0.9	41%	10.0 ± 1.8	3%
ΔC90-G103	14.2 ± 1.0	23%	N/A	6%

Figures

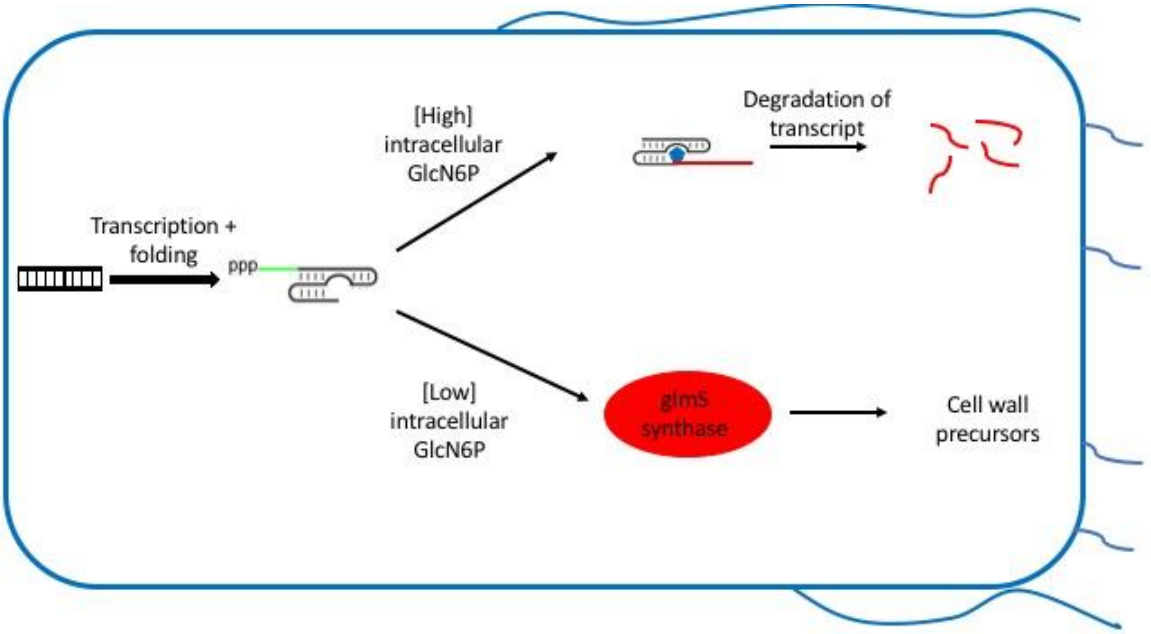

Fig 1: *glmS* regulation in gram positive bacteria. At low concentrations of glucosamine-6-phosphate (GlcN6P), *glmS* mRNA is translated to glmS synthase, which catalyzes the formation of metabolic precursors for the cell wall. At high concentrations, the ribozyme binds GlcN6P, initiating cleavage resulting in degradation of the downstream mRNA transcript.

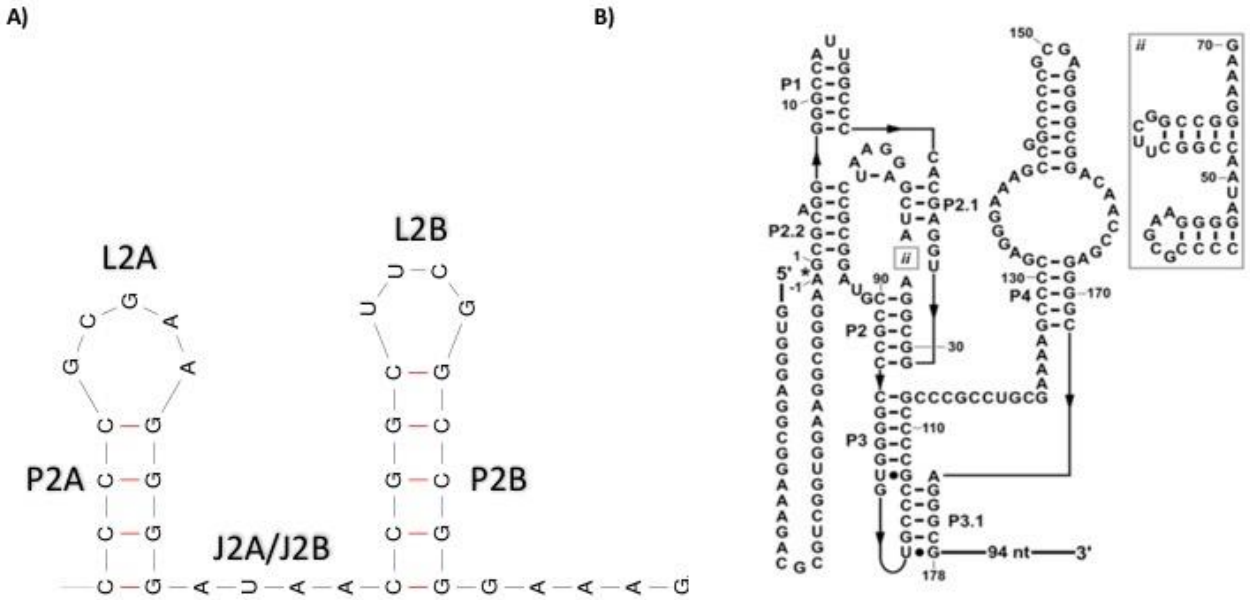

Fig 2: Predicted secondary structure of the additional module in *T. thermophilus*. **A)** Nomenclature of additional module. L2A denotes 5' loop and L2B denotes 3' loop containing UNCG motif. J2A/J2B denotes UAA triloop motif. **B)** Secondary structure of *glmS* ribozyme in *Thermus thermophilus*. Insert *ii* depicts the secondary structure of the additional module. "*An expanded collection and refined consensus model of glmS ribozymes*" (Breaker et al. 2011)

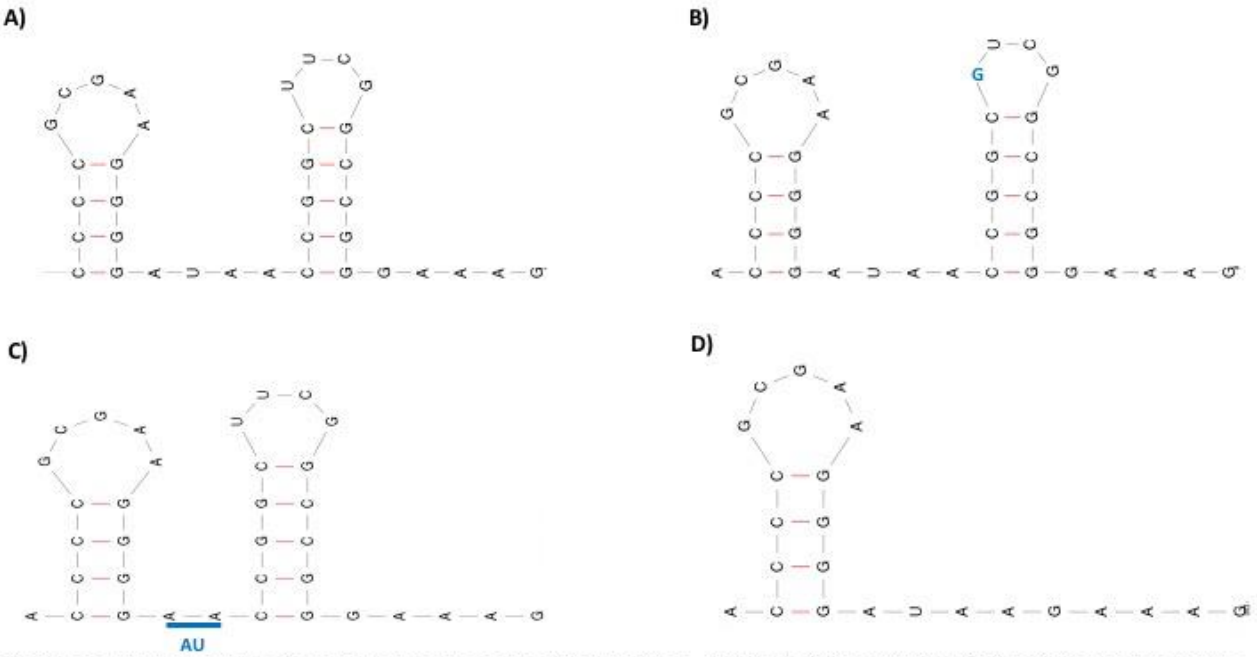

Fig 3: Secondary structures of additional module as predicted by mfold. **A)** WT **B)** U95G mutant. U → G mutation shown in blue **C)** A86delA87 mutant. **D)** C90delG103 deletion of entire 3' stem loop.

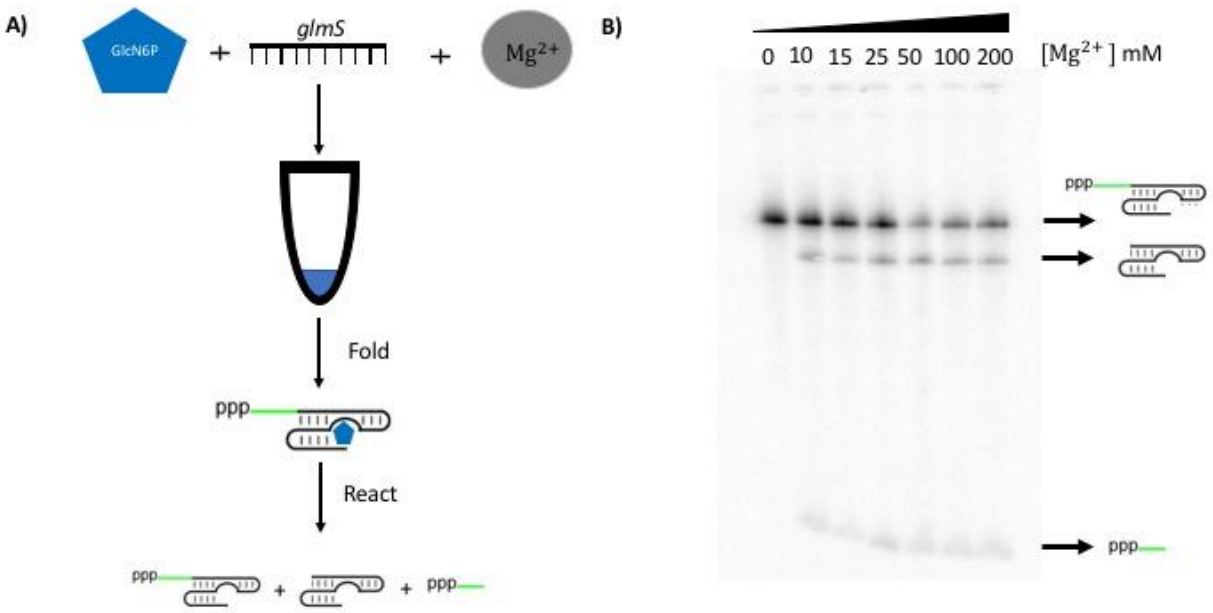

Fig 4: Setup of activity assays. **A)** Radiolabeled *glmS* RNA is added to 5 mM GlcN6P and varying [Mg^{2+}]. Reactions are folded at 37 °C for 5 min to fold the RNA, then reacted at 65 °C for 5 min. Urea denaturing dye added to quench reaction. **B)** Gel of WT *glmS* showing increasing activity with increasing Mg^{2+} concentration. Separation of products via denaturing 8% PAGE.

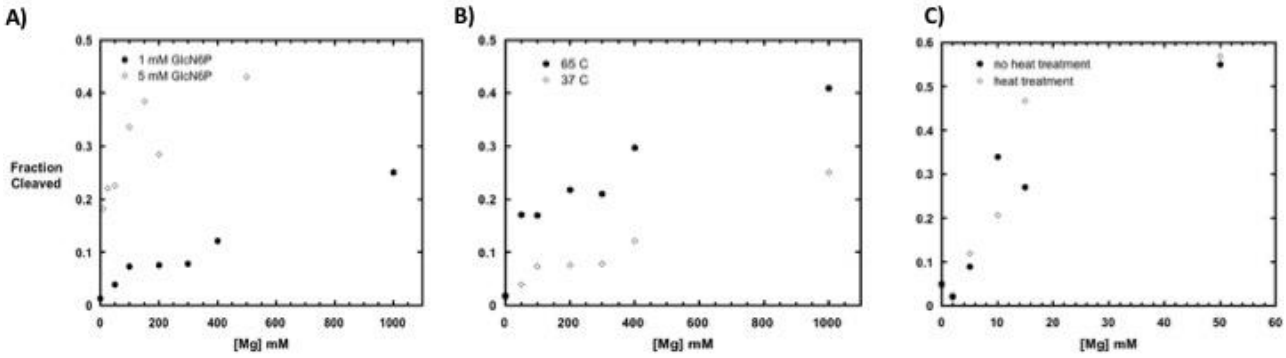

Fig 5: Optimization of reaction conditions for the WT *glmS* ribozyme. **A)** Fraction cleaved increases with ligand (GlcN6P) concentration. **B)** Higher fraction of ribozyme cleaves at 65 °C than 37 °C. **C)** incubating at 80 °C before folding had no effect on the fraction of *glmS* ribozyme that underwent self cleavage.

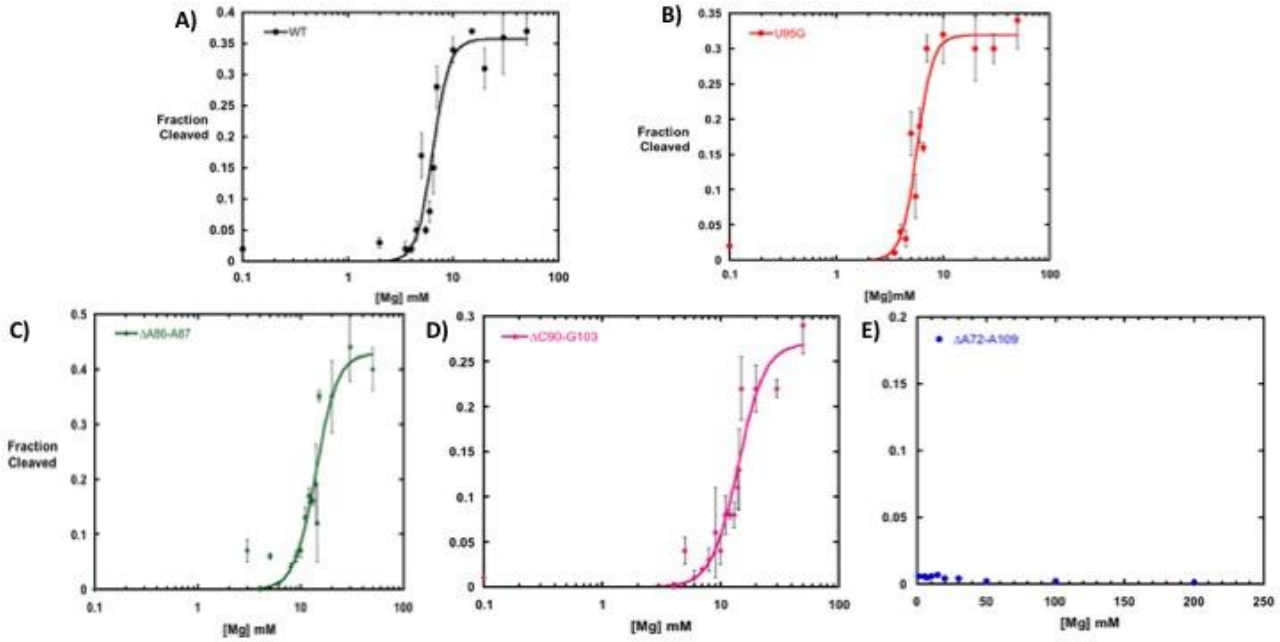

Fig 6: *glmS* activity as a function of $[Mg^{2+}]$. All assays were conducted in triplicate at 65 °C. Panels A-D were fit with the Hill equation to determine $Mg_{1/2}$ values. Errors bars represent standard of deviation.

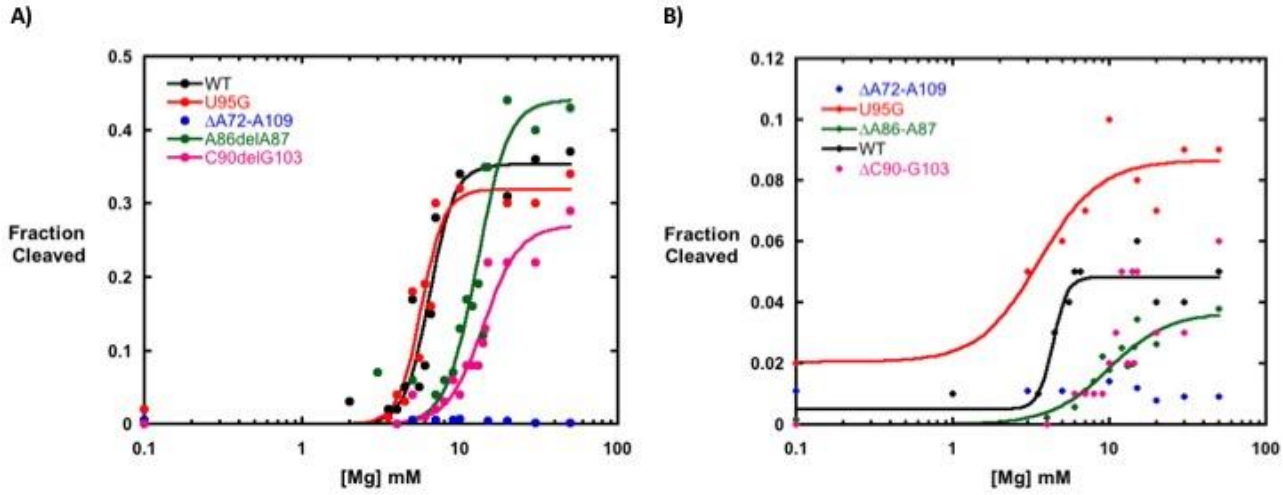

Fig 7: Activity of *glmS* at 65 °C and 42 °C. **A)** Maximal cleavage of WT and mutants occur at high temperature (65 °C). **B)** Cleavage activity of WT and mutants is significantly reduced at low temperature (42 °C).

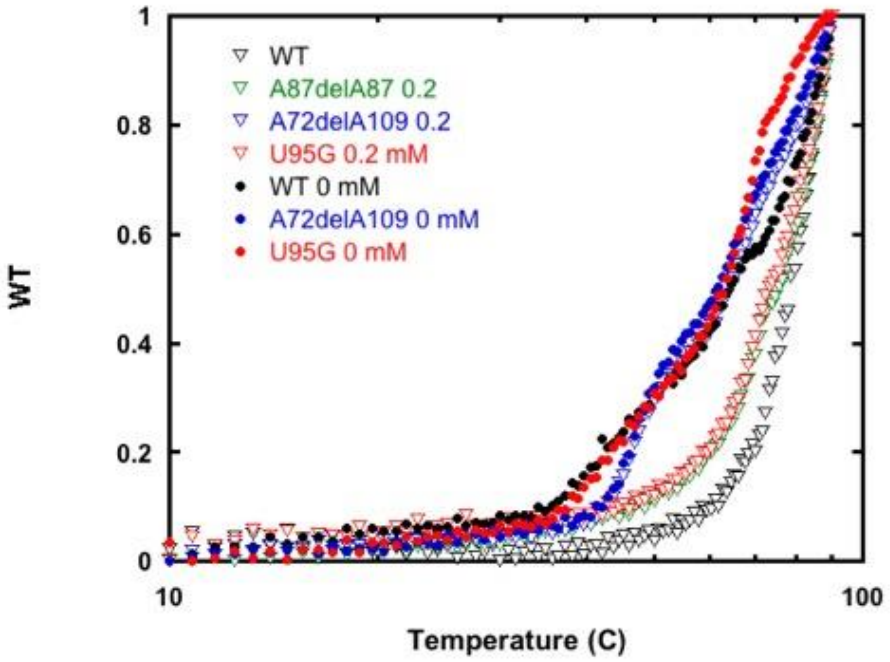

Fig 8: Thermal denaturation curves of all *glmS* ribozyme variants. The melting point, T_m, is increased with the addition of Mg^{2+} for all variants except ΔA72-A109.

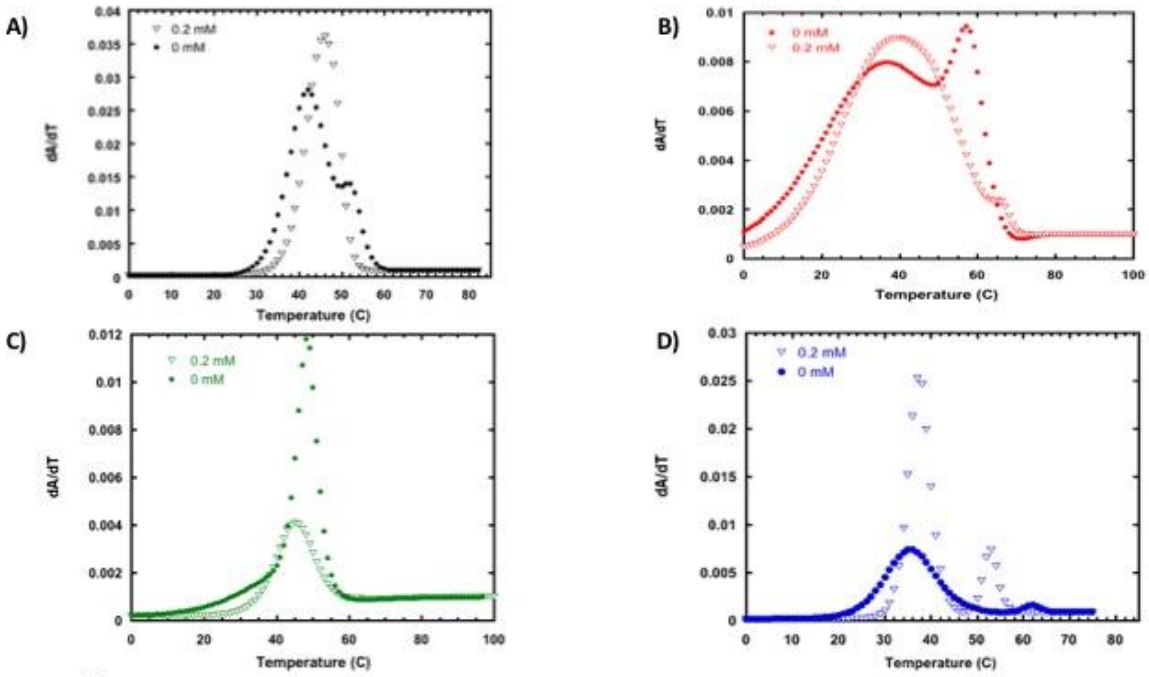

Fig 9: Plotting $\frac{\partial A}{\partial T}$ as function of temperature for *glmS* ribozyme variants. Peaks indicate T_m for each variant. **A)** WT **B)** U95G **C)** ΔA86-A87 **D)** ΔA72-A109

Introduction

The central dogma of biology emerged slowly, with early work focusing on the bookends of DNA and protein. Understanding of protein's role in cellular processes came first. Work by Eduard Buchner in 1897 identified yeast extract was capable of fermenting sugar, a catalytic process, in the absence of any living yeast cells[1]. Yeast extract was a mixture of proteins and other molecules, but in 1930 James Sumner, John Northrop, and Wendell Stanley proved that pure proteins alone could function as enzymes[2]. Collectively these discoveries led to the belief that protein was both the agent of catalysis as well as the source of genetic material. However, experiments by Hershey and Chase in 1952 confirmed DNA, not protein, contained the genetic information for all living things[3], and a year later the structure of DNA was solved by Watson and Crick[4]. Thus, the dogma evolved to one in which DNA contains the genetic information for all living things and proteins serve as the functional tools of that information. The role of RNA was relegated to that of a messenger, functioning solely as a temporary intermediate between information and action. Relatively recent discoveries like self-splicing RNAs, metabolite sensing riboswitches, and the focus of this thesis, catalytic ribozymes, have upended this view.

Before the discovery of ribozymes, nucleic acid was regarded as a store of information while protein catalyzed chemical reactions. The discovery of a self-splicing ribosomal RNA in *Tetrahymena* was identified provided the first evidence to the contrary[5]. Soon after, another catalytic RNA, ribonuclease P, was discovered in *Escherichia coli*[6]. These concurrent discoveries suggested a multitude of enzymatic

activities may be associated with RNA.

Besides catalysis, RNA fulfills other roles within the cell that have traditionally ascribed to protein. *In vitro* selection experiments in the 1990's showed that RNA could bind metabolites and proteins[7,5]. These experiments suggested that, like protein, RNA could sense the concentration of intracellular metabolites, and respond to changing conditions in a regulatory manner. Given that many biological processes make use of the same metabolites, metabolite binding RNAs should be a conserved regulatory theme *in vivo*.

Metabolite binding RNAs were first identified *in vivo* in the early 2000's[8,6]. These unique RNAs were termed riboswitches for their ability to modulate genetic expression. Each riboswitch is composed of two components; an aptamer which binds the metabolite, and an expression platform which undergoes a structural change upon metabolite binding[9]. The structural changes of the expression platform regulate transcription or translation. At the level of transcription, riboswitches switch between Rho-independent terminators or an anti-terminator hairpin to regulate expression[10]. Riboswitches regulating gene expression at the level of translation function via occlusion or release of ribosome binding sites[11]. These mechanisms create a regulatory network in which the concentration of a metabolite directly influences gene expression.

A regulatory framework increases the complexity of the RNA world, but to function reproducibly the riboswitches governing that framework must have a high specificity for their ligand. Activation of a riboswitch by alternative ligands would jeopardize the proper function of the regulatory network. This specificity is a function of the RNA sequence itself. Single-stranded RNA forms a secondary structure determined

by canonical Watson-Crick base pairing. Base pairing regions form stems, while non-base paired regions form loops. The formation of secondary structure gives rise to a higher order tertiary structure. Tertiary structure is governed by interactions, such as base stacking, backbone hydrogen bonding, long range interactions between loops to form pseudoknots, and tetraloop-tetraloop receptor pairs[12]. The RNA structural elements that combine to form these tertiary interactions are well defined and highly conserved[13]. Searching for conserved sequences that contain similar motifs could therefore be used as a method to identify new riboswitches.

This type of systemic search led to the discovery of the *glmS* ribozyme in *B. subtilis*. A series of intergenic regions in the *B. subtilis* genome that produced highly structured RNA domains had been identified[14]. Those same sequences were highly conserved between bacterial species and formed complex folded structures[15]. This indicated that these intergenic regions contained a highly-structured RNA, similar to a riboswitch, that was catalytically active and conserved across bacterial species. The riboswitch candidate lay directly upstream of an essential gene, which encodes GlmS synthase, an enzyme that utilizes fructose-6-phosphate (F6P) and glutamine to generate glucosamine-6-phosphate (GlcN6P)[16](Fig. 1A). The presence of a highly structured RNA upstream of a key gene in a biochemical pathway strengthened the hypothesis that the RNA is a riboswitch, and may bind a metabolite produced either directly or indirectly by the downstream gene, resulting in regulation of that gene. Winkler et. al confirmed *glmS* is a riboswitch, and is regulated by GlcN6P, the product generated by GlmS synthase[17].

glmS interacts with a metabolite to regulate translation, thus meeting the definition of a riboswitch. However, rather than occlude the ribosome binding site, the

glmS ribozyme prevents translation by self-cleavage of the transcript itself, leading to its subsequent degradation by ribonuclease J1[18]. As GlcN6P is produced by F6P synthase the intracellular concentration of GlcN6P rises, increasing the likelihood that the metabolite will interact with the glmS mRNA. Binding of GlcN6P to glmS catalyzes a transesterification reaction that is initiated by a 2' OH attack on a phosphorous atom of the adjacent phosphodiester bond[19]. Cleavage generates two products: a shorter leader sequence and the remaining transcript, which now starts with a 5' OH group. The 5' OH group is the substrate for RNase J1[18], which degrades the mRNA preventing translation (Fig 1A). Disruption of *glmS* ribozyme function via mutations to the active site *in vivo* in *E. coli* led to loss of sporulation and an inability to form a biofilm[18]. The loss of sporulation and biofilm formation phenotypes generated interest in the *glmS* ribozyme as a possible antibiotic target. Identification of an agonist for the ribozyme would prevent translation of GlmS synthase, preventing cellular division.

The search for an agonist of the *glmS* ribozyme continued with the work of McCown et al. who utilized a bioinformatics approach to identify 463 possible *glmS* ribozyme representatives based upon their similarity to a consensus sequence and the known crystal structure of the *glmS* ribozyme in *Bacillus subtilis*, a mesophilic bacterium[20]. Five *glmS* ribozyme candidates had an altered core structure containing additional structural elements. In one of these bacteria, the hot spring dwelling thermophile *Thermus thermophilus*, the *glmS* ribozyme contains an additional module with multiple structural elements with RNA tertiary motifs[20]. The module is comprised of two stem-loops, P2A and P2B, held together with a short linker sequence J2A/J2B (Fig. 2A). It is likely that the additional module, located close to the core (Figure 2B), protects

the function of the ribozyme, and therefore the regulation of an essential gene, at the high temperatures found within a hot spring.

A high temperature environment affects the structure of RNA by increasing the overall kinetic energy of a system[21]. Increased motion leads to the disruption of long range tertiary interactions, and as temperature increases, eventual loss of hydrogen bonding within a structure[22]. In the case of the *glmS* ribozyme, the RNA's structure is required for proper function[23]. To prevent a loss of function in high temperature environments, additional tertiary interactions are required to maintain the RNA's folded conformation.

Each of the conserved motifs in the additional module potentially facilitate formation of a tertiary interaction. The L2B loop is composed of a UNCG tetraloop motif, where N refers to any nucleotide and R refers to a purine (Figure 2A). The UNCG motif is the most common tetraloop motif in RNA, and one of the most thermostable[24]. The 3' loop is connected to the 5' loop by a three base pair (UAA) triloop (J2A/J2B, Fig 2A), and hydrogen bonding between the UA base pairs may play a role in regulating spacing between each of the stems. In each thermostable species, the additional module always ends in GAAAR[25], which potentially interacts with another region to stabilize the ribozyme.

I hypothesize that the additional module forms tertiary interactions that increase the stability of the ribozyme at high temperature. Specifically, the L2A and L2B stem-loops and the joining region, J2A/J2B (Fig. 2A), between them is required to create tertiary contacts that stabilize the core region and preserve function at high temperatures. Changes to L2B and J2A/J2B may destabilize the tertiary structure, preventing the

ribozyme from efficiently self-cleaving. A decrease in cleavage activity in mutated versions of the ribozyme would suggest the additional element supports cleavage activity at high temperature through tertiary interactions. The effect of those tertiary interactions on stability will be assayed using thermal denaturation to map the unfolding of the *glmS* ribozyme as temperature increases. Together the results of activity assay and thermal denaturation experiments will be used to determine if loss of cleavage activity is a result of decreased stability at high temperature.

Methods

Preparation of *glmS* synthetic gene

A synthetic gene was created using the genomic sequence of *glmS* in *T. thermophilus* specified by McCown et al (NCBI reference sequence number, NC_006461.1). The position of *glmS* within the sequence is between positions 1781664-1781865[26]. This genomic sequence was expanded by adding nucleotides on the 5' end to assist in separation of the products post-cleavage on denaturing acrylamide gel. Restriction enzyme sites were added at 5' and 3' ends to facilitate linearization of pDNA when desired (Scheme 1). The *glmS* sequence ordered as a synthetic gene from Integrated DNA Technologies (IDT) and was inserted into pUC19. The ampicillin resistance gene was included to select for transformed bacteria. M13 forward and reverse sites were included for later sequencing. Henceforth this construct is referred to as pthermo (Scheme 2).

Scheme 1

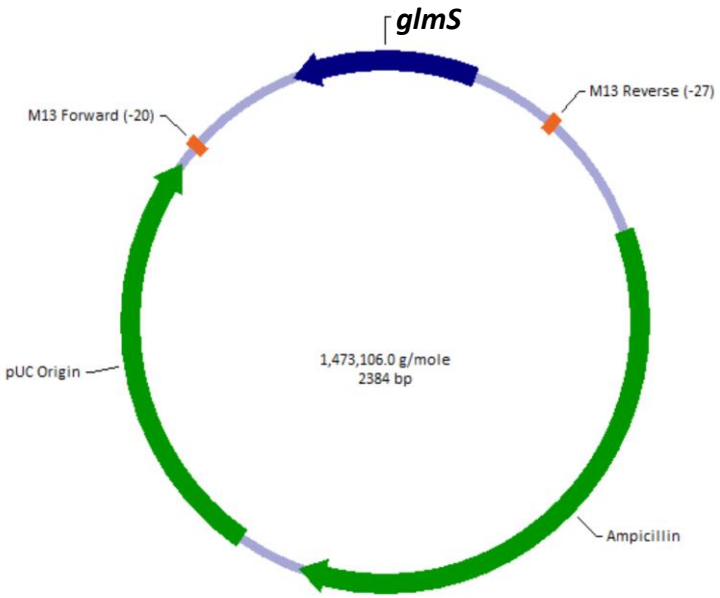

Scheme 2

***pthermo* plasmid purification**

pthermo (10 ng) was transformed into DH5α cells (C2987H) from New England Biolabs (NEB) using High Efficiency Transformation Protocol (C2987H/C2987I) available from the NEB. After transformation, bacterial growths were diluted 10-fold in LB. Then 50 µL of the 1:10 dilution mixture was plated onto .1 mg/L ampicillin selective agar. Plates were incubated at 37 °C overnight. The following day single

colonies were picked and transferred to 5 mL LB with 1x ampicillin. Cultures were grown at 37 °C in a shaker overnight. The 5 mL culture was added to a 500 mL large scale culture the following day and grown overnight at 37 °C in shaker. Plasmid DNA was extracted using a Qiagen Maxiprep Kit and accompanying protocol and run on a 1% agarose gel to check purity.

Restriction enzyme digest of pthermo

To create a template for run-off transcription pthermo DNA was linearized using BamH1-HF (NEB). 10 μg pthermo was digested at a time in 500 μL reactions. 10 μg pthermo was added to 50 μL 10x NEB Cutsmart Buffer, 3 μL BamH1-HF, and nanopure (np) H_2O to 500 μL. Reactions were digested at 37 °C overnight. Digested DNA was run on a 1% agarose gel to ensure complete digestion and correct plasmid size.

Targeted mutagenesis of *glmS*

Four different mutations were introduced to the *glmS* ribozyme, creating four specific variants; U95G, ΔA86-A8, ΔC90-G103, and ΔA72-A109. Two mutations, U95G and ΔA86-A87, were introduced by Quikchange mutagenesis using primers designed by Agilent Technologies© Quikchange© Primer Design. This program generated primers that would result in a single base change (U95G) or a small deletion (ΔA86-A87). Primers for quickchange mutants, U95G and ΔA86-87, were used in a PCR reaction with pthermo template. This amplification reaction produced pDNA containing the desired

mutation. The remaining two mutants, ΔA72-A109, and ΔC90-G103 were larger deletions, and were engineered using inverse PCR. These primers were designed such that the 5' ends leave a region unbound while 3' ends extend outward in opposite directions (scheme 3). The plasmid from amplification contains a targeted deletion within the *glmS* sequence.

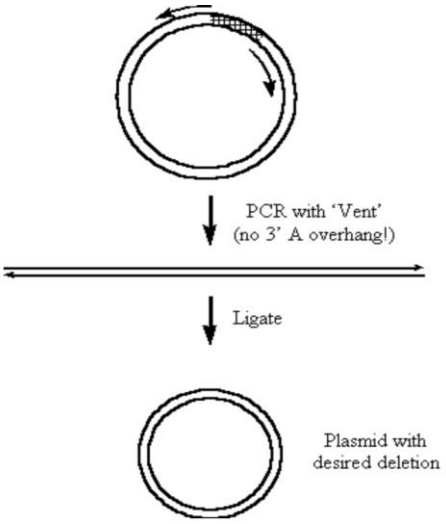

Dr. Michael Blauber. Univeridade Federal Do Rio Grande Sol

Scheme 3

Mutated pthermo DNA for all mutants was transformed into DH5α (NEB) component cells, plated on ampicillin selective media, and several colonies were cultured. The pthermo DNA from these cultures was then extracted and sequenced using M13 reverse primer to confirm the presence of the desired mutations.

Introduction of T7 consensus sequence via PCR

For efficient transcription using the T7 promoter, the first few transcribed nucleotides must be GGAGG. To increase efficiency of transcription an altered T7 promoter region was required that encoded a T7 consensus sequence. This sequence was introduced via PCR reaction. A primer containing the T7 consensus sequence and reverse *glmS* primer were used in a 200 μL PCR reaction with linearized pthermo as template, generating *glmS* PCR DNA in sufficient quantities to use in *in vitro* transcriptions.

Preparation of radiolabeled pre-RNA

To visualize and quantify the cleavage reaction, the uncleaved *glmS* RNA was radiolabeled via incorporation of α-^{32}P ATP during *in vitro* transcription. Linearized template pthermo (750 ng) was transcribed in a 30 μL *in vitro* transcription reaction containing 1x *glmS* buffer, 1x low ATP-NTP buffer, 60 μCi α^{32}P ATP, and 1 μL of T7 RNA polymerase. Reactions were incubated at 37 °C for 30 minutes. An equal volume of 2x TBE denaturing dye was added and RNA products were separated using 8% denaturing polyacrylamide gel electrophoresis (PAGE). RNA was excised from the gel and extracts recovered by soaking the gel fragment in 10 mM HEPES pH 7.6, EDTA 1 mM, and KCl 250 mM overnight. RNA was precipitated by adding sodium acetate to a final concentration of 300 mM (pH 5) and 2 volumes of cold 100% ethanol, and stored at -80 °C for 30 min. RNA was then pelleted by centrifugation, and the resulting pellet was washed in 300 μL 70% ethanol to remove residual salts. The pellet was dried by vacuum

and suspended in 50 μL HE buffer (25 mM HEPES, 1 mM EDTA).

Mg^{2+} titrations with radiolabeled RNA

1500 counts internally $^{32}P-$ labeled RNA was added to a 10 μL reaction containing 50 mM HEPES-KOH pH 7.6, 200 mM KCl, and 5 mM GlcN6P. 1 μL of 10x Mg^{2+} was added and the reaction was spun down. Reactions were incubated at 37 °C for 5 minutes to allow the ribozyme to fold, followed by a 5 minute incubation at 65 °C for the cleavage reaction to occur. An equal volume of 2x TBE dye was added and the reaction was spun down. 2 μL of each reaction was loaded into denaturing 8% PAGE and separated by running the gel at 15 W until the bromophenol dye reached the bottom of the gel (approximately 1 hour). The gels were then dried and imaged.

Quantification of Mg^{2+} Titrations

Images were visualized using a Storm 820 PhosphorImager and PhosphorImager storage cassettes. Quantification was preformed using ImageQuant (v5.2). For each RNA species individual bands were defined by a box of identical size for each RNA species (cleaved, 5' leader, uncleaved). After background subtraction the total number of counts for each reaction was the sum of the counts from the three RNA species (cleaved, 5' leader, uncleaved). Outliers were defined as any reaction which had a total number of counts outside one standard of deviation from the average of the total counts for all reactions in an experiment, were excluded from further analysis. The fraction cleaved for each sample was then defined as $\frac{\text{Cleaved}}{\text{Uncleaved+Cleaved+Leader}}$ expressed as a percentage and

plotted against Mg^{2+} concentration. The data were fit using the Hill equation $\theta = (M)\frac{(\frac{G}{P})}{1+(\frac{G}{P})^2}$ where M is the maximal fractional cleaved, G is an empirical parameter corresponding to the $[Mg^{2+}]$, and P is the midpoint of the transition.

Error analysis for activity assays

Each data point in all activity assays reflects the average of three experiments. Error bars within each plot represent one standard of deviation from this average. Uncertainty in the half-maximal Mg^{2+} concentration, $Mg_{1/2}$, is calculated by fitting each activity assay to the Hill equation defined previously.

Large scale transcription of *glmS*

10 μg *glmS* PCR DNA was transcribed in a 1 mL in vitro reaction containing 1x *glmS* buffer, 5 mM of each of the four ribonucleoside 5' triphosphates (NTPs), 0.2 U of yeast inorganic phosphatase (NEB), and 20 μL T7 polymerase. Reactions were incubated at 37 °C for three hours. An equal volume of 2x TBE denaturing dye was added and RNA products were separated using 8% denaturing polyacrylamide gel electrophoresis (PAGE). RNA was excised from the gel and recovered by soaking the gel fragment in TEN buffer (10 mM Tris-HCl pH 7.5, 1 mM EDTA, 250 mM NaCl) overnight. Salt was removed using Amicon Ultra 3000 NMW microconcentrators. Equal volumes of eluate from overnight rocking and 200 mM Tris-HCl pH 7.5 were added to the column (total volume 20 mL). The column was centrifuged for 15' at 4000 x g in JS 5.3 rotor. After

spinning, the column is removed and flow through discarded. After initial spin 20 mM Tris-HCl pH 7.5 was added to column to increase volume to 20 mL. The column was then centrifuged for 15' at 4000 g in JS 5.3 rotor. This process of adding 20 mM buffer, spinning, and discarding flowthough was repeated five times to ensure removal of salt from the RNA. After five spins RNA was concentrated down to ~500 µL by spinning under same parameters without adding additional buffer. Final RNA concentration was determined using Thermofisher Nanodrop-1000 spectrophotometer.

Thermal denaturation experiments

Thermal denaturation experiments were performed using an Aviv 14DS UV-Vis spectrophotometer. For each experimental sample, a blank containing only buffer was also prepared. Each sample (or blank) had a total volume of 1 mL with 50 mM HEPES-KOH pH 7.6, 10 µM EDTA and 0.2 mM $MgCl^{2+}$, with or without the experimental RNA at a concentration of 20 ng/µL (OD 0.6). Quartz 1 cm pathlength cuvettes were used. The absorbance of each sample was measured at 405nm, 295nm, 280nm, and 260nm. Absorbance measurements were taken as the temperature was increased in 0.8 °C increments from 23 °C to 90 °C. Once each desired temperature was reached, the sample was equilibrated at that temperature for 1 minute. Five absorbance readings were taken for at each wavelength and the average was recorded. For ease of visualization each denaturation curve is presented as a plot of the first derivative of absorbance at a specified wavelength with temperature with respect to temperature (dA/dT). Derivatives were calculated using Global Melt Fit, a software program written by David Draper to

extract thermodynamic information from multi-transition UV data[27]. This program was updated by Anthony Mustoe. By plotting the first derivative against the temperature, transitions are revealed as peaks in the melting profile, with the apex of each peak marking the T_m.

Results

Design and preparation of *glmS* ribozyme mutants

To test the hypothesis that the additional module ensures function at high temperature, mutations were engineered to target tertiary motifs within the additional module. If the hypothesis is correct, and additional module stabilizes the ribozyme at high temperature through increasing the number of tertiary interactions, then loss or perturbation of these interactions will decrease the functionality of the ribozyme. Therefore, each mutation was designed to destabilize a predicted tertiary interaction within the additional module of the *glmS* ribozyme. Mutant U95G is a single base change in L2B. In WT *glmS* (Fig. 3A) L2B is a UNCG tetraloop motif in which U1-G4 form a wobble base pair, while C3 base stacks with U1. By mutating the U position to G (Fig. 3B) both of these stabilizing interactions in the tetraloop are potentially disrupted. UNCG tetraloops are extremely stable at high temperature and can serve as nucleation sites for folding[28]. Disruption of the base stacking interaction within L2B via targeted mutagenesis may be enough to perturb that functionality.

The remaining mutations were deletions of varying size. ΔA72-A109 is a deletion

of the entire additional module, removing any stabilizing interactions it may be involved in. ΔA86-A87 is a two-base pair deletion in J2A/J2B between the P2A and P2B stem loops (Fig. 3C). ΔC90-G103 is a deletion of the P2B stem-loop (Fig. 3D). ΔC90-G103 removes the entire UNCG tetraloop, as well as the attached stem. Both ΔC90-G103 and ΔA86-A87 delete regions that are conserved among thermophilic bacteria, and are therefore likely to have a deleterious effect on ribozyme activity at high temperature.

Each of the four mutant sequences, U95G, ΔC90-G103, ΔA72-A109, and ΔA86-A87, the sequence of the additional module was run in mFold[29], a nucleic acid folding and hybridization prediction software, to predict the secondary structure of the module after mutation. These mutants were then used to examine the effect of lost tertiary interactions on the *glmS* ribozyme activity.

Optimization of wild type *glmS* activity

Before determining the effect of mutations on *glmS* activity, a baseline for WT *glmS* activity was established. This required the optimization of reaction conditions for the ribozyme. Parameters investigated included the presence or absence of monovalent and divalent salts, the reaction temperature, the conditions for folding, the concentration of ligand, the length of reaction time, and heat treatment before loading the reaction.

The presence of monovalent and divalent salts was critical to activity. Monovalent KCl is required to stabilize the negative charges within the phosphodiester backbone of the RNA. The electrostatic repulsion between these negative charges is relieved by the addition of positively charged potassium, which balances the forces of electrostatic

repulsion, allowing the RNA to fold[30]. Folding of the RNA is further facilitated by the addition of divalent Mg^{2+} which stabilizes the negatively charged phosphorous backbone at a lower entropic cost, as each Mg^{2+} ion balances the charges from two phosphorous ions[31]. Maximal activity of the ribozyme required 200 mM KCl and 50 mM $MgCl^{2+}$ (Fig. 4B.

Higher temperatures and increased concentration of GlcN6P also increased activity of the ribozyme. Before reactions were conducted, the ribozyme was folded at 37 °C in the presence of KCl and $MgCl^{2+}$. Afterwards folding, the ribozyme was reacted at either high (65 °C) or low (37 °C) temperature. Activity increased at higher temperature, and higher GlcN6P concentration (5 mM)(Fig. 5A, B). Increasing the length of reaction time past three minutes or heat treating the ribozyme before the folding step did not increase the activity of the ribozyme (Fig. 5C). Based upon these experiments, the optimal conditions for *glmS* ribozyme activity were established as described in the Methods (Mg^{2+} titrations with radiolabeled RNA).

Mutations destabilize tertiary interactions, necessitating higher [Mg^{2+}] for activity

Two criteria were used to quantify the effect of each mutation on *glmS* ribozyme activity. The first was the maximal extent of cleavage; at the highest Mg^{2+} concentration tested (50 mM). The second criterion was the Mg^{2+} concentration needed to reach half maximal magnesium concentration, $Mg_{1/2}$ The value of $Mg_{1/2}$ reflects the stability of the folded ribozyme and allows for stability comparisons between mutants that have different maximal rates of cleavage. By calculating both maximal cleavage and $Mg_{1/2}$, the

absolute and relative activity, and therefore stability, of each mutant can be compared.

Using magnesium concentration as a measure of the stability of the tertiary structure is based upon decades of previous work[32]. The phosphodiester backbone of RNA contains an abundance of repulsive negative charges. In order to form a folded tertiary structure, cations are required to neutralize those charges to a level at which weaker interactions, like base stacking and tetraloop/tetraloop receptor pairing, can overcome those repulsive forces. Divalent Mg^{2+} ions stabilize the tertiary structure of RNA in this manner[33]. Magnesium possesses a 2^+ charge and small atomic radius, which allows it to intercalate within the secondary structure and neutralize charges effectively, facilitating folding[34]. These characteristics make magnesium a requirement for formation of tertiary structure in many RNAs[35]. The dependency on RNA for magnesium to form tertiary structures makes half maximal magnesium concentrations ($Mg_{1/2}$) an effective measurement of how deleterious a mutation is to the stability of the ribozyme. Higher values of $Mg_{1/2}$ indicate more destabilizing mutations, while lower values of Mg^{2+} indicate a less significant change to the tertiary structure.

To compare the effects of the mutations on *glmS* ribozyme activity, the extent of self-cleavage was assayed as a function of increasing Mg^{2+} concentration. Radiolabeled RNA was folded in the presence of salts and reacted at 65 °C (Fig. 4A), and the fraction of RNA cleaved versus Mg^{2+} was fit to the Hill equation. The WT *glmS* ribozyme remained inactive until a concentration of 5 mM Mg^{2+} was reached. At that point, the ribozyme entered a steep transition region (Hill coefficient = 5.5) before reaching plateau at 15 mM Mg^{2+}(Fig. 6A). The $Mg_{1/2}$ of the WT ribozyme was 6.4 $\pm$ 0.4 mM Mg^{2+} (Table 1).

Mutant U95G shows a similar transition region to the WT, with $Mg_{1/2}$ = 5.7 $\pm$ 0.3 mM Mg^{2+} (Fig 6B), as well as a sharp transition region (Hill coefficient = 5.9). Both the WT and U95G have a similar level of maximal cleavage, 37% to 33% respectively (Table 1). Point mutation in the UNCG tetraloop (U95G) therefore did little to perturbed the tertiary structure in a manner that affected the ability of ribozyme to bind GlcN6P and react.

While the single base change of U95G had a mild effect on *glmS* ribozyme structure, the deletion mutants exhibited a more significant phenotype. ΔA72-A109 is a deletion of the entire additional module. Removal of the additional module abrogated the ability of *glmS* ribozyme to cleave at 65 °C (Fig. 6E). After correcting for background signal, cleavage was less than 0.019%, indicating a total loss of activity. Not all deletion mutants were as detrimental. ΔC90-G103, which removed P2B, still retained activity at 65 °C (Fig. 6D). However, ΔC90-G103 required a higher concentration of $Mg^{2+}$to initiate cleavage. The $Mg_{1/2}$ for ΔC90-G103 =14.2, twice the WT value (Table 1), and maximal cleavage was reduced to 23% (Fig. 6D). Together these results indicate that the loss of the P2B eliminates a tertiary interaction required for the function of the ribozyme. Higher Mg^{2+} concentrations restore some lost function to the ribozyme, but are not sufficient to restore WT activity.

Mutant ΔA86-A87 exhibited a combination of phenotypes. The $Mg_{1/2}$ is similar to ΔC90-G103 = 12.9 mM (Table 1), suggesting the loss of a supporting structural element. Unlike ΔC90-G103, ΔA86-A87 achieved WT activity at high Mg^{2+} concentrations with maximal cleavage reaching 41% (Fig. 6C). The shift in the $Mg_{1/2}$ is striking, given that ΔA86-A87 is a two-base pair deletion, yet is almost as destabilizing as

the removal of the P2B (Fig. 7A). While this deletion is destabilizing at low Mg^{2+} concentrations, higher concentrations of Mg^{2+} force ΔA86-A87 *glmS* ribozyme into a folded and active conformation. This folded conformation is not accessible by ΔC90-G103, which never reaches the WT level of activity.

All *glmS* variants are less active at 42 °C

T. thermophilus is adapted for growth in a high temperature environment (65 °C) [36], with one of those adaptions being the additional structural module in *glmS* ribozyme. Mutations that disrupt the stabilizing tertiary contacts of that module are deleterious to ribzyme activity at high temperature (ΔA86-A87, ΔC90-G103, ΔA72-A109). At lower temperatures, where the stability of the ribozyme is not as robustly challenged by the external environment, these mutations may not compromise its function. To test this hypothesis, activity assays with WT and MT *glmS* ribozymes were repeated at 42 °C. All ribozyme variants had reduced levels of activity at 42 °C (Fig. 7B). WT, U95G, and ΔA86-A87 all exhibited higher levels of activity with increasing Mg^{2+} concentrations while ΔC90-G103 showed no discernable relationship between Mg^{2+} concentration and activity. Interestingly, ΔA72-A109 continued to remain entirely inactive at 42 °C. The lack of activity by any *glmS* ribozyme variant suggests that rather than simply stabilize the core region at high temperature, the additional module participates in folding the ribozyme into an active conformation. Changes to the module prevent the ribozyme from adopting the active fold, leading to decreased activity.

Addition of Mg^{2+} increases the melting point of most *glmS* ribozyme variants

Each *glmS* ribozyme variant was thermally denatured in the absence or presence of Mg^{2+} (concentration 0.2 mM). For every variant except the whole deletion, ΔA72-A109, the addition of Mg^{2+} resulted in an increase the melting point (Fig. 8). An additional increase in UV absorption at very high temperature likely corresponds to the unfolding of the RNA secondary structure. It was not possible to assign a T_m for this trantransition because the secondary structure was not completely unfolded at 100 °C. Transition because the secondary structure was not completely unfolded at 100 °C. The magnitude of the shift in melting point due to Mg^{2+} ranged between *glmS* ribozyme variants. The WT *glmS* ribozyme experienced the most dramatic shift, with the T_m increasing from 41 °C to 49 °C (Fig. 9A). The T_m of ΔA86-A87, the two-base pair deletion in the J2A/J2B region increased from 43 °C to 49 °C (Fig. 9C) Variant U95G experienced a shift in T_m that was identical ΔA86-A87, increasing from to 49 °C (Fig. 8). In addition to exhibiting similar melting points in the presence of Mg^{2+}, U95G and ΔA86-A87 were previously characterized by the ability to achieve a WT level of self-cleavage in the presence of high concentrations of Mg^{2+}.

The only variant that did not experience a shift in melting point with the addition of Mg^{2+} was ΔA72-A109. At 0.2 mM Mg^{2+} ΔA72-A09 showed no change in the melting point. The $T_m$was also lower than the WT as well as all other ribozyme variants at 38°C (Fig. 9D). This fits with the activity data, which showed ΔA72-A109 possessed no self-cleavage activity.

Discussion

In Gram positive bacteria the *glmS* ribozyme is prefolded in the absence of ligand[37]. This is unusual, as most ribozymes and riboswitches are only partially folded, with ligand binding initiating a conformational change into the active state[38]. Prefolding confers high specificity to *glmS* ribozyme; self-cleavage requires addition of correctly structured amine containing ligands[39]. Other metabolites lacking the amine group in the proper orientation and chemical environment will fail to initiate cleavage. In contrast to Gram-positive bacteria, some Gram-negative bacteria regulate the *glmS* ribozyme allosterically[40]. In these examples, binding of GlcN6P to the ribozyme initiates a conformational change that induces self-cleavage activity. Whether *glmS* from *T. thermophilus* is prefolded or allosterically modified by GlcN6P binding has not been studied. My results provide evidence that *glmS* in *T. thermophilus* is prefolded, and that the additional module assists in proper folding of the ribozyme at high temperature, rather than preventing denaturation at high temperature.

All *glmS* variants experienced reduced activity at 42 °C except for ΔA72-A109, the whole module deletion. ΔA72-A109 was inactive at both 65 °C and 42 °C, proving that the additional module is required for activity. My hypothesis was that this module created additional tertiary contacts that stabilized the ribozyme structure under denaturing (high temperature) conditions. If that was the case then ΔA72-A109 should have still been active at 42 °C. At this lower temperature the additional tertiary contacts are not required to preserve the function of the ribozyme, and self-cleavage activity should be

intact. The observed complete loss of activity in ΔA72-A109 at 42 °C could be explained by a failure of the ribozyme to fold into an active conformation without the additional module. This is supported by the thermal denaturation data, which demonstrates that the addition of Mg^{2+}has no effect on the melting point of ΔA72-109. If ΔA72-A109 could form a folded structure then the stabilizing effect generated by that folded structure would have been detected in the thermal denaturation experiment.

Failure to properly fold into an active state could also explain the differences in the activity of the ΔC90-G103 and ΔA86-A87 ribozymes compared to the WT RNA. At 65 °C both of these variants required higher $Mg_{1/2}$ concentrations for activity compared to the WT *glmS* ribozyme. However, at the highest Mg^{2+}concentrations there was a marked difference in activity between ΔC90-G103 and ΔA86-A87. ΔA86-A87 displayed activity on par with the WT *glmS* ribozyme, with a maximal activity of 41%. In contrast, ΔC90-G103 maximal activity was half that level at 23%. This suggests that increased Mg^{2+}concentration forced ΔA86-A87 into an active folded conformation, but not ΔC90-G103, in which a higher proportion of the RNA remained in an inactive conformation. Thermal denaturation data shows that ΔA86-A87 does fold in the presence of Mg^{2+}, and has a T_m nearly identical to U95G. Both U95G and ΔA86-A87 achieved WT levels of self-cleavage. The evidence that they are similarly stabilized by Mg^{2+} indicates that there is likely a relationship between the ability of U95G and ΔA86-A87 ability to fold and their ability to undergo self-cleavage.

For both ΔC90-G103 and ΔA86-A87, this inactive state was the majority population at 42 °C. At low temperature ΔC90-G103 had a maximum cleavage of 6% while ΔA86-A87 only 3% of total RNA cleaved. The WT *glmS* ribozyme also

experienced a drop in activity, with only 5% of the RNA cleaving at 42 °C. The inactivity of the WT *glmS* ribozyme at 42 °C compared to 65 °C indicate that higher temperatures convert a population of inactive folded RNA to actively folded RNA that can react with GlcN6P. WT, ΔA86-A87, and ΔC90-G103 all had a similar basal level of cleavage, indicating that some of the RNA in each variant was able to fold into an active conformation, however this was a rare subpopulation. Unfortunately no thermal denaturation data was gathered on ΔC90-G103. Difficulties in preparing adequate supplies of RNA meant only a single experiment could be run, and in a shockingly poor bit of luck, the lamp in the spectrophotometer burned out in the middle of the experiment.

In conclusion, the hypothesis that tertiary contacts made by the additional module are stabilizing the catalytic core of the *glmS* ribozyme is an incomplete way of describing the role of the additional structure. While it is unknown if the *glmS* ribozyme is prefolded in *T. thermophilus*, these data suggest that the tertiary contacts made by the additional module are assisting in guiding the ribozyme into an active folded state. Removal of the module abrogates activity at 65 °C as well as 42 °C. High Mg^{2+}concentrations restore the activity of variants containing small deletions (ΔA86-A87), but not larger ones (ΔC90-G103). Changes that did not delete base pairs, and disrupted base stacking interactions instead (U95G) slightly reduced maximal activity, but did not shift $Mg_{1/2}$ concentrations. Similar levels of activity at 42 °C across all variants indicate that a small population of RNA always folds into an active conformation, but temperature itself plays an important role in folding the ribozyme correctly. While further experiments are required to confirm *glmS* in *T. thermophilus* is prefolded, this data suggests that the additional module creates tertiary contacts that assist in folding the ribozyme into an active state at 65 °C.

The *glmS* ribozyme functions at the intersection of metabolism and genetic regulation. As a master switch for an essential gene, there can be no room regulatory error. This evolutionary pressure has produced a structured RNA that is highly specific for GlcN6P. My data indicate that the formation of such a specific active site requires a highly coordinated folding process. Perturbations as small as two base pairs (ΔA86-A87), hamper the ribozymes ability to fold at a physiologically relevant Mg^{2+}concentration. Understanding the elements critical to functional folding of the *glmS* ribozyme, both in thermophilic and mesophilic bacterial species, is a requirement before any agonist molecule could be developed. This work contributes to that task by suggesting that the *glmS* ribozyme in *T. thermophilus* is prefolded.

Appendix

Each header below corresponds to a section of text within the methods. Under each header relevant sequence data has been included to assist in potentially repeating any of the above experiments.

glmS synthetic gene

GAATTTC: EcoR1
TAATA: T7 promoter
GGATCC: BamH1

GAATTCTAATACGACTCACTATAGG**GTGGGAGGCGGAAAGACGCGTCG**GT
GGAAGGCGGGAA*GCGCGGGGGCCATTGGCCCCACGAGGTGGCGGACCCCG
CGAAGGGGATAACCGGCTTCGGCCGGGAAAGATCGAGGAATCCGCGGATGC
CGCCCGGGGTGTGCCCGCCCCGCCCGCCTGCGAAAAGCCCCGAGGGAAAGCC
GGCCCCGCGAGGGGCGGACAACCGAGGGGCAGGGCGGGATCC

Bolded nucleotides were added for ease of separation on denaturing gel
*denotes cleavage site
Underlined nucleotides are from NCBI reference genome NC_006461.1

Primers for targeted mutagenesis of *glmS*

Point Mutations (quickchange)

U95G (U95G)

5’ CCGGCGTCGGCCGGGAAAGATC forward
5’ GCCGGTTATCCCCTTCGCGG reverse

A86 to A89 (ΔA86-A87)

5’ gaagccggttcccttcgcggggtc
5’ gaccccgcgaaggggaaccggcttc

Deletion of Additional Module (inverse PCR)

Deletion from C73 to A109 (ΔA72-A109)

5’ TCGAGGAATCCGCGGATGCCG
5’ TCCGCCACCTCGTGGGGCCAAT

Deletion of 3’ loop (inverse PCR)

Deletion from C90 to G103 (ΔC90-G103)

5’ GAAAGATCGAGGAATCCGCGG
5’ TTATCCCCTTCGCGGGGTCC

Introduction of T7 consensus sequence via PCR

T7_Forward primer: 5’ TAATACGACTCACTATAGGGAGGCGGAAAGACGCGT

T7_Reverse primer: 5’ CCGCCCTGCCCCTCGGTTGT

Preparation of radiolabeled pre-RNA

glmS buffer

Item	Volume (uL)
500 mM HEPES pH 7.5	2500
250 mM MgCl2	1250
100 mM DTT	500
20 mM Spermidine-HCl	100
.1% triton X-100	5
npH20	675

References

[1] "Eduard Buchner – Nobel Lecture: Cell-Free Fermentation". *Nobelprize.org*. 1907.
[2] "Nobel Prizes and Laureates: The Nobel Prize in Chemistry 1946". *Nobelprize.org*.
[3] HERSHEY, A. D., & CHASE, M. (1952). Independent functions of viral protein and nucleic acid in growth of bacteriophage. *The Journal of General Physiology*, *36*(1), 39–56.
[4] WATSON, J. D., & CRICK, F. H. C. (1953). Molecular Structure of Nucleic Acids: A Structure for Deoxyribose Nucleic Acid. *Nature*, *171*(4356), 737–738. http://doi.org/10.1038/171737a0
[5] Kruger, K., Grabowski, P. J., Zaug, A. J., Sands, J., Gottschling, D. E., & Cech, T. R. (1982). Self-splicing RNA: autoexcision and autocyclization of the ribosomal RNA intervening sequence of Tetrahymena. *Cell*, *31*(1), 147–157.
[6] Guerrier-Takada, C., Gardiner, K., Marsh, T., Pace, N., Altman, S. Cell 35, 849 (1983)
[7] Ellington, A.D., and Szostak, J.W. (1990). In vitro selection of RNA molecules that bind specific ligands. Nature *346*, 818–822
[5] Robertson, D.L., and Joyce, G.F. (1990). Selection *in vitro* of an RNA enzyme that specifically cleaves single-stranded DNA. Nature *344*, 467–468
[8] Mironov, A. S., Gusarov, I., Rafikov, R., Lopez, L. E., Shatalin, K., Kreneva, R. A., et al. (2002). Sensing small molecules by nascent RNA: a mechanism to control transcription in bacteria. *Cell*, *111*(5), 747–756.
[6] Nahvi, A., Sudarsan, N., Ebert, M.S., Zou, X., Brown, K.L., and Breaker, R.R. (2002). Genetic control by a metabolite binding mRNA. Chem. Biol. *9*, 1043– 1049.
[9] Serganov, A., & Nudler, E. (2013). A decade of riboswitches. *Cell*, *152*(1-2), 17–24. http://doi.org/10.1016/j.cell.2012.12.024
[10] Trausch, J. J., & Batey, R. T. (2015). Design of modular "plug-and-play" expression platforms derived from natural riboswitches for engineering novel genetically encodable RNA regulatory devices. *Methods in Enzymology*, *550*, 41–71. http://doi.org/10.1016/bs.mie.2014.10.031
[11] Johnson, J. E., Reyes, F. E., Polaski, J. T., & Batey, R. T. (2012). B12 cofactors directly stabilize an mRNA regulatory switch. *Nature*, *492*(7427), 133–137. http://doi.org/10.1038/nature11607
[12] Hendrix, D. K., Brenner, S. E., & Holbrook, S. R. (2006). RNA structural motifs: building blocks of a modular biomolecule. *Quarterly Reviews of Biophysics*, *38*(03), 221–23. http://doi.org/10.1017/S0033583506004215
[13] Hermann, T., & Patel, D. J. (2000). Adaptive recognition by nucleic acid aptamers. *Science (New York, N.Y.)*, *287*(5454), 820–825.
[14] Soukup, G. A. & Breaker, R. R. Relationship between internucleotide linkage geometry and the stability of RNA. *RNA* **5**, 1308−1325 (1999)
[15] Vitreschak, A. G., Rodionov, D. A., Mironov, A. A. & Gelfand, M. S. Riboswitches: the oldest mechanism for the regulation of gene expression? *Trends Genet.* **20**, 44−50 (2004)
[16] Milewski, S. Glucosamine-6-phosphate synthase: the multi-facets enzyme. *Biochim. Biophys. Acta* **1597**, 173−192 (2002)
[17] Winkler, W. C., Nahvi, A., Roth, A., Collins, J. A., & Breaker, R. R. (2004). Control of gene expression by a natural metabolite-responsive ribozyme. *Nature*, *428*(6980), 281–286. http://doi.org/10.1038/nature02362
[18] Collins, J. A., Irnov, I., Baker, S., & Winkler, W. C. (2007). Mechanism of mRNA destabilization by the glmS ribozyme. *Genes & Development*, *21*(24), 3356–3368. http://doi.org/10.1101/gad.1605307
[19] Klein, D. J., & Ferré-D'Amaré, A. R. (2006). Structural basis of glmS ribozyme activation by glucosamine-6-phosphate. *Science (New York, N.Y.)*, *313*(5794), 1752–1756. http://doi.org/10.1126/science.1129666
[13] Collins, J. A., Irnov, I., Baker, S., & Winkler, W. C. (2007). Mechanism of mRNA destabilization by the glmS ribozyme. *Genes & Development*, *21*(24), 3356–3368.
[13] Collins, J. A., Irnov, I., Baker, S., & Winkler, W. C. (2007). Mechanism of mRNA destabilization by the glmS ribozyme. *Genes & Development*, *21*(24), 3356–3368.
[20] McCown, P. J., Roth, A., & Breaker, R. R. (2011). An expanded collection and refined consensus model of glmS ribozymes. *Rna*, *17*(4), 728–736. http://doi.org/10.1261/rna.2590811
[20] McCown, P. J., Roth, A., & Breaker, R. R. (2011). An expanded collection and refined consensus model of glmS ribozymes. *Rna*, *17*(4), 728–736. http://doi.org/10.1261/rna.2590811

[21] Narberhaus, F., Waldminghaus, T., & Chowdhury, S. (2006). RNA thermometers. *FEMS Microbiology Reviews*, *30*(1), 3–16. http://doi.org/10.1111/j.1574-6976.2005.004.x
[22] Chen, Y. Z., & Prohofsky, E. W. (1996). Sequence and temperature effect on hydrogen bond disruption in DNA determined by a statistical analysis. *European Biophysics Journal : EBJ*, *25*(1), 9–18.
[23] Lau, M. W. L., & Ferré-D'Amaré, A. R. (2013). An in vitro evolved glmS ribozyme has the wild-type fold but loses coenzyme dependence. *Nature Chemical Biology*, *9*(12), 805–810. http://doi.org/10.1038/nchembio.1360
[24] Sheehy, J. P., Davis, A. R., & Znosko, B. M. (2010). Thermodynamic characterization of naturally occurring RNA tetraloops. *Rna*, *16*(2), 417–429. http://doi.org/10.1261/rna.1773110
[25] McCown, P. J., Roth, A., & Breaker, R. R. (2011). An expanded collection and refined consensus model of glmS ribozymes. *Rna*, *17*(4), 728–736. http://doi.org/10.1261/rna.2590811
[26] McCown, P. J., Roth, A., & Breaker, R. R. (2011). An expanded collection and refined consensus model of glmS ribozymes. *Rna*, *17*(4), 728–736. http://doi.org/10.1261/rna.2590811
[27] Draper DE, Bukhman YV, Gluick TC. Thermal Methods for the Analysis of RNA Folding Pathways. In: Beaucage SL, Bergstrom DE, Glick GD, Jones RA, editors. Current Protocols in Nucleic Acid Chemistry. section 11.13. John Wiley & Sons; New York: 2000. p. 13.
[28] M. Molinaro, I Tinoco. Use of ultra-stable UNCG tetraloop hairpins to fold RNA structures: thermodynamic and spectroscopic applications. Nucleic Acid Residues 1995. , *23*(15), 3056–3063.
[29] Zuker, M. (2003). Mfold web server for nucleic acid folding and hybridization prediction. *Nucleic Acids Research*, *31*(13), 3406–3415.
[30] Draper, D. E. (2004). A guide to ions and RNA structure. *Rna*, *10*(3), 335–343. http://doi.org/10.1261/rna.5205404
[31] Misra, V.K., Shiman, R., and Draper, D.E. 2003. A thermodynamic framework for the magnesium-dependent folding of RNA. *Bio- polymers* **69:** 118–136
[32] Stein, A., & Crothers, D. M. (1976). Conformational changes of transfer RNA. The role of magnesium(II). *Biochemistry*, *15*(1), 160–168. http://doi.org/10.1021/bi00646a025
[33] Shiman, R., & Draper, D. E. (2000). Stabilization of RNA tertiary structure by monovalent cations. *Journal of Molecular Biology*, *302*(1), 79–91. http://doi.org/10.1006/jmbi.2000.4031
[34] Woodson, S. A. (2010). Compact intermediates in RNA folding. *Annual Review of Biophysics*, *39*(1), 61–77. http://doi.org/10.1146/annurev.biophys.093008.131334
[35] Stein,A. and Crothers,D.M. (1976) Conformational changes of transfer RNA. The role of magnesium(II). *Biochemistry*, **15**, 160–168.
[36] Yuki Hidaka, Masumi Hasegawa, Tadaatsu Nakahara & Takayuki Hoshino (1994) The Entire Population of Thermus thermophilus Cells Is Always Competent at Any Growth Phase, Bioscience, Biotechnology, and Biochemistry, 58:7, 1338-1339, DOI: 10.1271/bbb.58.1338
[37] Hampel, K. J., & Tinsley, M. M. (2006). Evidence for Preorganization of the glmS Ribozyme Ligand Binding Pocket †. *Biochemistry*, *45*(25), 7861–7871. http://doi.org/10.1021/bi060337z
[38] Winkler, W. C., and Breaker, R. R. (2005) Regulation of bacterial gene expression by riboswitches, *Annu. Re*V. *Microbiol. 59*, 487- 517.
[39] McCarthy, T. J., Plog, M. A., Floy, S. A., Jansen, J. A., Soukup, J. K., & Soukup, G. A. (2005). Ligand Requirements for glmS Ribozyme Self-Cleavage. *Chemistry & Biology*, *12*(11), 1221–1226. http://doi.org/10.1016/j.chembiol.2005.09.006
[40] Kalamorz, F., Reichenbach, B., März, W., Rak, B., & Görke, B. (2007). Feedback control of glucosamine-6-phosphate synthase GlmS expression depends on the small RNA GlmZ and involves the novel protein YhbJ in Escherichia coli. *Molecular Microbiology*, *65*(6), 1518–1533. http://doi.org/10.1111/j.1365-2958.2007.05888.x

C U R R I C U L U M V I T A E

James Cameron
Born March 8, 1994. Boston, Massachusetts
M.S. Program, The Johns Hopkins University, Baltimore, MD

Research Experience

2014-present Member of Dr. Sarah Woodson's laboratory. The Johns Hopkins University Department of Biophysics. Currently conducting independent research on the structure of the *GlmS* ribozyme in *T. thermophilus*. Project focuses on the role tertiary interactions in stabilizing the catalytic core of the ribozyme. These interactions allow *T. thermophilus* to retain activity at high temperature.
http://biophysics.jhu.edu/woodson/index.html

Education

2016-2017 Expected graduation date May 2017. Earning a M.S. degree in Molecular and Cellular Biology.

2016 B.S. Molecular and Cellular Biology, The Johns Hopkins University, Baltimore, MD.

Honors and awards

2015-2016 Dean's List (GPA of 3.5 or higher) for fall and spring semesters.

Professional Societies

2016 Teaching Assistant for Biochemistry Laboratory. Guided 14 students through 11 labs focusing on different aspects of biochemistry. Responsible for grading lab reports and exams, as well as holding regular office hours.

2017-Present Teaching Assistant for General Biology Lab. Guided 24 students through 12 labs designed to introduce fundamental topics in molecular biology, physiology, and anatomy.